JOURNAL OF MODERN OPTICS, 1998, VOL. 45, NO. 2, 299–314

Modified conventional plane-wave scattering approach to estimate performance characteristics of laser particle-size analysers*

V. I. OVOD

Particle Sizing Systems, 75 Aero Camino, Santa Barbara, CA 93117 and Department of Chemistry, University of California, Santa Barbara, CA 93106, USA

M. STINTZ

Institut für Verfahrenstechnik, Technische Universität Dresden, Mommsenstraße 13, D-01062 Dresden, Germany

E. HEIDENREICH

IFF Forschungsinstitut Futtermitteltechnik Frickenmühle, D-38110 Braunschweig-Thune, Germany

(*Received 7 March 1997; revision received 29 May 1997*)

Abstract. A technique is derived for the rapid engineering simulation of the influence of the main instrumental parameters of a laser particle-size analyser on its response function and other main performance characteristics. The technique is based on the modified conventional (classical) plane-wave approach. From the methodological point of view, this method incorporates a set of nondimensional coefficients describing the change of the amplitude, duration and shape of a pulsed signal for different particle trajectories in a Gaussian beam with a circular or elliptical cross-section. The above-mentioned performance characteristics as well as the distortion of the signal shape caused by the bandwidth limitation of a photodetector are investigated taking into account the nondimensional coefficients. It was shown that the technique is valid for the modelling of measurements of attenuation and/or near-forward scattering by single particles in the broad practical range of particle diameters. Correctness of the modified technique has been confirmed experimentally and theoretically by comparison with the exact generalized Lorenz-Mie theory. Application of the technique for the rapid investigation of performance characteristics of laser particle-size analysers is illustrated.

Nomenclature

- a instrumental parameter
- c shape factor of a Gaussian beam
- f nondimensional time characterizing the nondimensional coordinate of a particle along the X axis

* Correspondence should be addressed to V. I. Ovod

new kinds of commercial analysers and their improvement and modification for different applications in manufacturing industries have been of prime interest to many scientific and engineering teams [1–4]. It is well known that most performance parameters and characteristics of any analyser depend on the so-called response function, which shows the attenuation or scattering of the laser radiation vs. the particle diameter.

For practical operations, an analyser is calibrated experimentally with primary size standards of known optical properties. On the other hand, the accurate and rapid simulation of response functions is of key importance [1–8] for any engineering design of new kinds of commercial analysers with improved performance characteristics and for the automatic correction of results in real time of measurements, if optical properties of measured particles differ from the optical properties of calibrated lattices.

Most of the techniques developed for the above calculations use the classical ray optics approach [5] or the rigorous Mie scattering algorithm [6–9]. Both algorithms, which are valid for the plane-wave light source only, give sufficient calculation errors if the diameter of a particle is significantly larger than the dimension of a laser spot.

Recent achievements in calculation techniques (for example, the generalized Lorenz–Mie theory [10–13] and the theory of the angular spectrum of plane waves (PWS) [14, 15]) make it possible to provide exact calculations of the scattering of a focused Gaussian beam by particles. Being a powerful tool for the exact simulation of response functions, these techniques are not optimal for engineering simulations and for use in the software of laser analysers because of the huge calculation time.

The aim of this work is the adaptation of a modified conventional plane-wave approach for the rapid and accurate engineering simulation of the main performance characteristics of a laser particle-size analyser in the broad range of particle diameters. A set of nondimensional coefficients are proposed to simplify the simulations and for estimating the influence of the main instrumental parameters of an analyser and such factors as the nonuniformity of particle illumination and the bandwidth limitation of a photodetector on the response function of the analyser. Comparisons with the more exact generalized Lorenz–Mie theory and with experimental results lend support to the validity of the modified technique for the near-forward scattering and extinction measurement.

The authors hope that this technique may be useful for the rapid engineering optimization of the optical layout of a laser particle-size analyser. Techniques for the optimization of other units of analysers (a hydrodynamic chamber and a unit for space sorting of particles) have been published recently in [16, 17].

2. Generalized optical layout of a laser particle-size analyser

A generalized optical layout of a laser particle analyser is presented in figure 1. Let a Gaussian laser beam be propagated along the optical axis OZ of the particle analyser, being focused in the measurement zone (plane XOY) into an elliptical spot with the minor semi-axis ω_x and major semi-axis ω_y measured at the $\exp(-2)$ maximum intensity level. Using a special running-type chamber described, for example in [6, 16], the particles move at the velocity V in the direction that is parallel to the axis OX. Hence, the space position of a particle crossing the laser beam is characterized by corresponding coordinates $\{x_p = Vt, y_p, z_p\}$, where time t

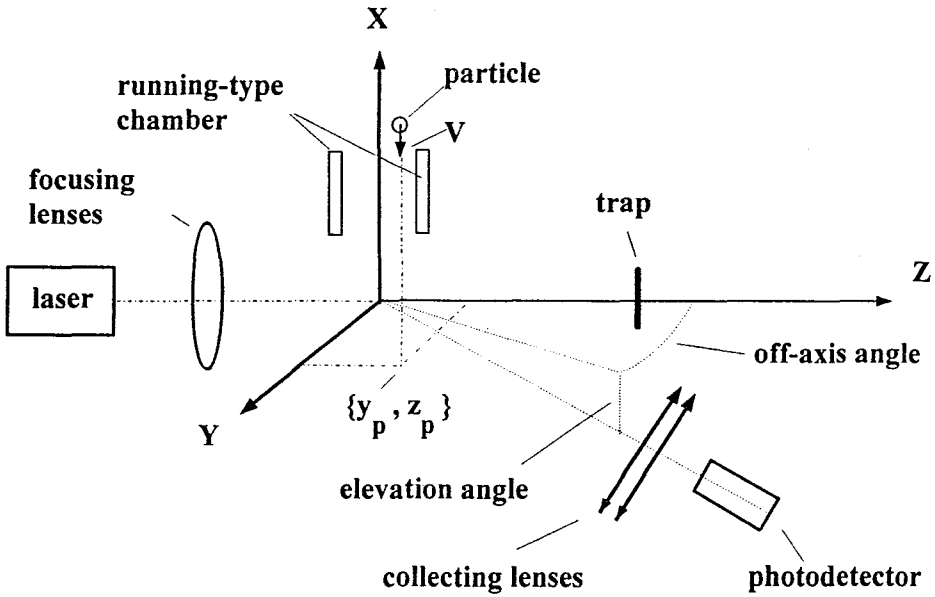

Figure 1. Optical layout of a laser particle-size analyser.

is measured from the moment at which the particle passes through the plane YOZ. A light attenuated or scattered by a moving particle in a near-forward direction is collected onto a photodetector by lenses. An absorbing trap is installed on the optical axis of the analyzer when the scattering light is detected. The trap protects the photodetector against the direct exposure of the laser beam.

Hence, the response function (calibration curve) of the particle analyser is the function of the signal amplitude (or the duration) through the radius of a particle.

An additional unit may be installed after the measurement zone for the space sorting of particles in real time taking into account their diameters [17].

3. Conventional plane-wave scattering approach

It is well known that Mie theory [6–9] is only rigorous for simulation of scattering by a spherical particle if the source of light is a plane-wave. According to this theory [9, Chap. 3.4 and Chap. 13.5], the light power P_μ attenuated ($\mu = \text{att}$) or scattered ($\mu = sca$) by a particle into the aperture Ω of a photodetector is determined by the expression:

$$P_{\mu\,\text{plane}}(\Omega, r) = I_{0\,\text{plane}}\sigma_{\mu\,\text{plane}}(\Omega, r), \tag{1}$$

where $I_{0\,\text{plane}}$ is the intensity of an illuminating plane-wave; $\sigma_{\mu\,\text{plane}}$ is the cross-section of a particle simulated by using the Mie plane-wave scattering theory [6–9]; r is the radius of the particle.

Equation (1) has been widely used in a conventional plane-wave approach for the estimation of the response function of a laser particle-size analyser in the range of particle diameters sufficiently less than the spot of a laser. To extend the range of investigated diameters and to estimate other performance characteristics of an analyser, this approach should be modified.

4. Modified conventional plane-wave scattering approach

As mentioned above, the angular spectrum of plane waves is a powerful tool for the rigorous simulation of scattering of an arbitrary beam by particles. According to this theory, an arbitrary illuminating field is expressed by the angular spectrum of the jth plane waves (PWS). Hence, the scattered field is presented as a superposition of the fields which are scattered by a particle illuminated by each jth plane wave from the above spectrum [14, 15].

For the rapid estimation of the power scattered by a particle, a modified conventional plane-wave approach may be used instead of PWS theory [18]. As follows from this approach, the above spectrum, depending on the beam characteristics, particle location, particle size, and its optical properties, may be replaced by a single plane wave corresponding to the spectrum. The wavelength λ of this plane wave in a medium should be equal to the wavelength of the real beam in the same medium (let us assume the illuminating beam be Gaussian), and the intensity I_{plane} of the plane wave should be chosen in such a manner that the radiation $P_{\text{c plane}}$ incident on the geometrical cross-section of a particle is similar to the radiation $P_{\text{c Gauss}}$ for the real beam:

$$I_{\text{plane}}(r, x_{\text{p}}, y_{\text{p}}, c(z_{\text{p}})) = \frac{P_{\text{c Gauss}}(r, x_{\text{p}}, y_{\text{p}}, c(z_{\text{p}}))}{\pi r^2}, \tag{2}$$

where

$$P_{\text{c Gauss}}(r, x_{\text{p}} y_{\text{p}}, c(z_{\text{p}})) = \int\int_{x^2+y^2 \leqslant r^2} I_{\text{Gauss}}(x - x_{\text{p}}, y - y_{\text{p}}, c(z_{\text{p}}))\, \mathrm{d}x\, \mathrm{d}y; \tag{3}$$

$$I_{\text{Gauss}}(x, y, z, c(z)) = \frac{2P_0}{\pi \omega_x^2(z) c(z)} \exp\left(-2\left(\frac{x^2}{\omega_x^2(z)} + \frac{y^2}{\omega_y^2(z)}\right)\right) \tag{4}$$

is the density of the laser Gaussian radiation flux in the measurement zone [19]; $c(z) = \omega_y(z)/\omega_x(z)$ is the shape factor of the Gaussian beam in the z cross-section; P_0 is the laser flux in the measurement zone.

In view of Eqs. (2)–(4), Equation (1) for a Gaussian beam can be written using nondimensional coefficients:

$$P_{\mu\,\text{Gauss}}(\Omega, r, t) = k_{\text{a}}(t = 0, l, s, c) k_{\text{sh}}(t, l, s, c) P_{\mu\,\text{plane}}(\Omega, r), \tag{5}$$

where

$$P_{\mu\ \text{plane}}(\Omega, r) = P_o k_{\text{a1}}(\mathrm{w}_x, c) \sigma_{1\mu\ \text{plane}}(\Omega, r); \tag{6}$$

$t = \omega_x f/(2V)$; $l = r/\omega_x$ and $f = 2x_{\text{p}}/\omega_x$, $s = 2y_{\text{p}}/\omega_x$ are the nondimensional radius of the measured particle and its coordinates, respectively;

$$k_{a1}(\omega_x, c) = \frac{1}{2c(z_{\text{p}})} \left(\frac{\lambda}{\pi \omega_x(z_{\text{p}})}\right)^2 \tag{7}$$

is the normalizing coefficient showing the influence of the Gaussian beam parameters on the amplitude of a detected signal (Eq. (7) coincides with the results obtained in [2] for the case of a circular cross-section);

$$k_{\text{sh}}(t, l, s, c) = \frac{k_{\text{a}}(t, l, s, c)}{k_{\text{a}}(t = 0, l, s, c)} \tag{8}$$

is the nondimensional coefficient describing the shape of a nondistorted time-dependent signal;

$$k_a(t=0,l,s,c)=\frac{c(z_p)}{2l^2}\frac{P_{c\,\mathrm{Gauss}}(t=0,f,s,c(z_p))}{P_0} \tag{9}$$

is the normalized coefficient considering the influence of the illumination non-uniformity of a particle on the steepness of the response function; $\sigma_{1\mathrm{sca\,plane}}(\Omega,r)$ and $\sigma_{1\mathrm{att\,plane}}(\Omega,r)=\sigma_{1\mathrm{ext\,plane}}(r)-\sigma_{1\mathrm{sca\,plane}}(\Omega,r)$ are the scattering and attenuation cross-sections of a particle in relative units calculated according to the plane-wave Mie scattering theory [9].

Nondimensional value of the cross-section $\sigma_{1\mu}$ correlates with the known ([9], chap. 3.4) cross-section σ_μ and with the corresponding effectiveness factor Q_μ:

$$\sigma_{1\mu}=\frac{4\pi\sigma_\mu}{\lambda^2},\quad \sigma_{1\mu}=Q_\mu\rho^2,\quad \sigma_\mu=\pi r^2 Q_\mu. \tag{10}$$

Considering Eqs. (3), (4) and (9), the following expression can be derived for the simulation of the relation $P_{c\,\mathrm{Gauss}}/P_o$ for an arbitrary location of a particle

$$\frac{P_{c\,\mathrm{Gauss}}(t,l,s,c)}{P^0}=\frac{1}{2\pi c}\exp\left(-\frac{c^2f^2+s^2}{2c^2}\right)\int_0^{2l}\int_0^{2\pi}\exp\left(-\frac{c^2+1}{4c^2}\rho^2\right)$$
$$\times\exp\left(\frac{1-c^2}{4c^2}\rho^2\cos 2\varphi\right)\exp\left(\frac{c^2f\cos\varphi+s\cos\varphi}{c}\right)\rho\,\mathrm{d}\rho\,\mathrm{d}\varphi, \tag{11}$$

where ρ and φ are the polar radius and angle, respectively. Equation (11) can be simplified for the next two symmetrical locations of the particle in the measurement volume and/or for the circular cross-section of a laser beam:

$$\frac{P_{c\,\mathrm{Gauss}}(t=0,l,s=0,c)}{P_0}=\frac{1}{c}\int_0^{2l}\exp\left(-\frac{c^2+1}{4c^2}\rho^2\right)I_0\left(\frac{c^2-1}{4c^2}\rho^2\right)\rho\,\mathrm{d}\rho; \tag{12}$$

$$\frac{P_{c\,\mathrm{Gauss}}(t,l,s=0;c=1)}{P_0}=\frac{P_{c\,\mathrm{Gauss}}(t=0,l,s,c=1)}{P_0}$$
$$=\exp\left(-\frac{\nu^2}{2}\right)\int_0^{2l}\exp\left(-\frac{\rho^2}{2}\right)I_0(\nu\rho)\rho\,\mathrm{d}\rho, \tag{13}$$

where $v=f$ when $s=0$, or $v=s$ when $t=0$; $I_0(u)$ is the zero-order Bessel function of an imaginary argument u;

$$\frac{P_{c\,\mathrm{Gauss}}(t=0,l,s=0;c=1)}{P_0}=1-\exp(-2l^2). \tag{14}$$

Hence, the time-dependent signal at a linear amplifier output can be determined by the following expression:

$$R_{\mathrm{ph\,Gauss}}(t,l,s,c)=R_{a\,\mathrm{Gauss}}(l,s,c,)k_{\mathrm{ph}}(t,l,s,c,), \tag{15}$$

where

$$R_{a\,\mathrm{Gauss}}(l,s,c)=k_\nu k_{al}\sigma_{1\mu\,\mathrm{Gauss}}(t=0,l,s,c) \tag{16}$$

is the amplitude of an ideal nondistorted signal;

$$\sigma_{1\mu\,\mathrm{Gauss}}(t,l,s,c)=k_a(t,l,s,c)\sigma_{1\mu\,\mathrm{plane}} \tag{17}$$

is the attenuation or scattering cross-section of a particle in a Gaussian beam;

$$k_\nu = k_0 k_{1a} P_0 \tag{18}$$

is the constant coefficient of linear units of an analyser; $k_0 = r_1 M S_c$ is the coefficient of signal conversion by a photodetector; r_1 is the load resistance of a photodetector; $M \geqslant 1$ is the amplification coefficient of a photomultiplier (when using a photodiode $M = 1$; S_c is the sensitivity of the photoreceiver cathode; $k_{1a} \geqslant 1$ is the amplification coefficient of a linear amplifier;

$$k_{ph}(t, l, s, c) = \frac{1}{t_{ph}} \int_0^\infty k_{sh}(t - \tau, l, s, c) \exp\left(-\frac{\tau}{t_{ph}}\right) d\tau \tag{19}$$

is the time-dependent coefficient in terms of the Duhamel integral allowing for estimating the distortion of the shape of a short signal caused by the bandwidth limitation of a photodetector; t_{ph} is the time constant characterizing the photodetector speed of response. Thus, the amplitude of a detected signal can be simulated by the equation

$$R_{a\,ph}(l, s, c) = R_a(l, s, c) k_\tau(l, s, c), \tag{20}$$

where

$$k_\tau(l, s, c) = \max\{k_{ph}(t, l, s, c)\} \tag{21}$$

is the coefficient of a pulse amplitude reduction.

5. Calculations

5.1. *Influence of the Gaussian beam parameters on the response function of the analyser*

5.1.1. *Calibration curve as a function of signal amplitude*

As follows from the analysis of equations (7) and (16), the coefficient k_{a1} makes possible the estimation of the influence of a laser beam shape on the amplitude of a signal. Figure 2 illustrates the quantitative decreasing of the signal amplitude with the increasing of the minor semi-axis ω_x and of the shape coefficient c (curves 1–4 correspond to $c = 1, 5, 10, 20$ respectively; $\lambda = 0{\cdot}6328$ μm) of a laser beam with an elliptical cross-section.

Investigation of the coefficient k_a (see equation (9)) is of interest because it shows the decrease in the steepness of response functions of an analyser in the range of particles with large diameters. This coefficient is presented in figures 3 and 4 vs. the nondimensional radius of particle $l = r/\omega_x$. Curves in figure 3 correspond to the different values of the shape coefficient of an elliptical beam when a particle is on the axis OZ (curves 1–4 are presented for $c = 1, 2, 10, 40$). Curves 1–4 in figure 4 are obtained for different positions of a particle in a circular laser beam (curves 1–4 correspond to $s = 0, 0{\cdot}6, 1, 1{\cdot}4, 2$).

The relation $P_{c\,Gauss}/P_0$ that enters into the coefficient k_a (see equation (9)) is the probability that a causal quantity (the intensity of a laser beam) characterized by two-dimensional normal distribution hits in a circular area (the geometrical cross-section of a particle). In general, the circular area (a particle) can be displaced relatively to the dispersion centre of the above quantity. The above-mentioned relation is given for different locations of a particle in a laser beam with the circular cross-section in figure 5 (curves 1–5 correspond to $s = 0, 0{\cdot}6, 1, 1{\cdot}4, 2$),

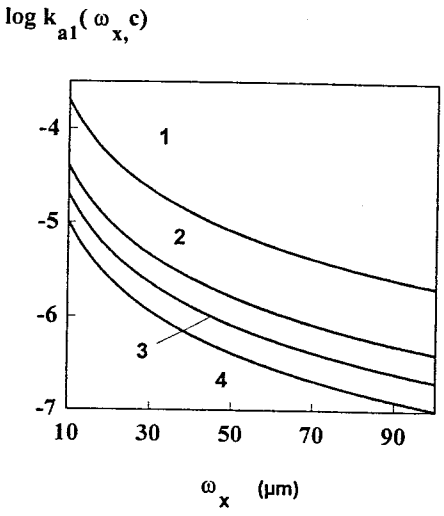

Figure 2. Coefficient k_{a1} showing the influence of the Gaussian beam parameters on the amplitude of a detected signal for $\lambda = 0{\cdot}6328\,\mu m$: curves 1–4 correspond to $c = 1$, 5, 10, 20, respectively.

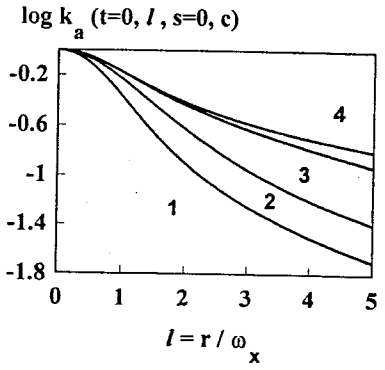

Figure 3. Influence of the shape coefficient of a laser beam on the response function of an analyser: curves 1–4 are presented for $c = 1$, 2, 10, 40.

and in figure 6 for the different shape coefficient of a laser beam with an elliptical cross-section (curves 1–7 are given for $c = 1$, 2, 5, 7, 10, 20, 40).

5.1.2. *Calibration curve as a function of signal duration*

Equation (19) can be simplified

$$k_{ph}(t, l, s, c) \simeq k_{sh}(t, l, s, c), \tag{22}$$

when a photodetector with a high speed of response is used. As follows from the analysis of the coefficient $k_{sh}(t, l, s, c)$ presented in figure 7 (curve 1 is plotted for very small particles $l \to 0$, and 2–4 are obtained for $l = 0{\cdot}5$, $0{\cdot}8$, 1, respectively), the shape of the nondistorted signal is close to a bell-shaped form.

As mentioned above, another kind of response function used for particle sizing is the dependence of the duration $\tau_L = f_L(l, s, c)\omega_x/(2V)$ of a pulsed signal on the

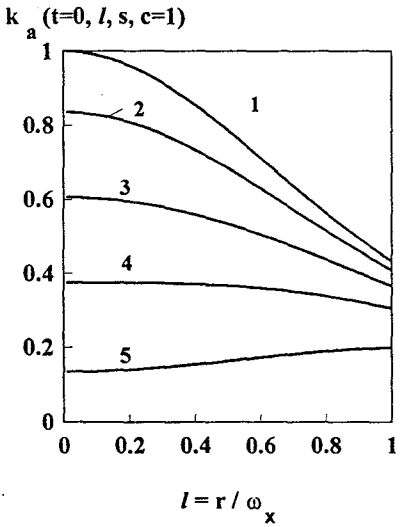

Figure 4. Influence of the particle position in a circular laser beam on the amplitude of the detected signal: curves 1–5 correspond to $s = 0$, 0·6, 1, 1·4, 2.

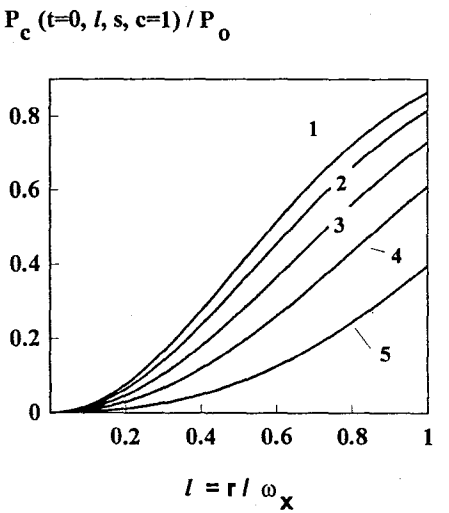

Figure 5. Power incident on the geometrical cross-section of a particle having different postions in the laser beam with a circular cross-section ($c = 1$): curves 1–5 correspond to $s = 0$, 0·6, 1, 1·4, 2.

diameter of the particle (where L is the level from the maximum amplitude of the signal). This kind of response function is shown in figure 8 for different values of the shape coefficient of a Gaussian beam (curves 1–3 correspond to $c = 1$, $c = 2$; $c \geqslant 10$).

Obviously, linearity of response functions is observed at $l \geqslant 1{\cdot}5$ and does not depend upon the material of particles. Good agreement between these theoretical and experimental results (the experimental results published first in [20] for $c = 24$ are plotted in figure 8 as curve (filled circles)) confirm the correctness of the proposed simplified technique.

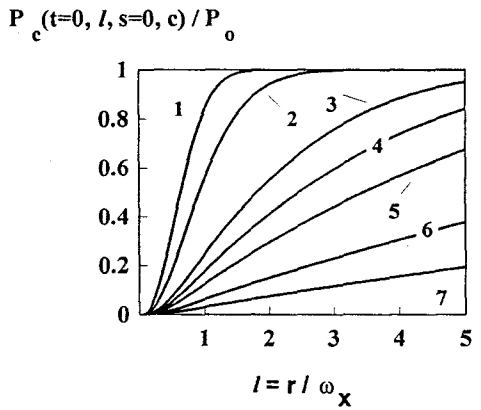

Figure 6. Power incident on the geometrical cross-section of a particle located in the centre of a laser beam with a circular (1) and elliptical cross-section (2–7): curves 1–7 correspond to $c = 1, 2, 5, 7, 1\text{-}, 20, 40$.

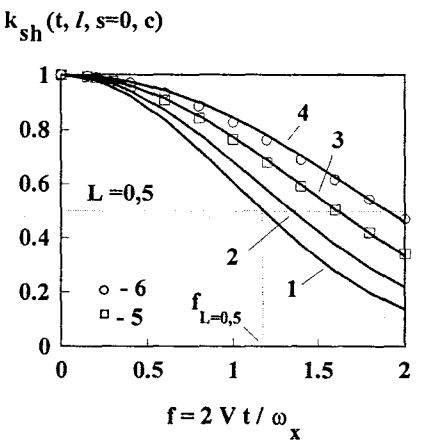

Figure 7. Normalized nondistorted signal detected from particles with nondimensional radius $l \to 0$ (curve 1) and $l = 0{\cdot}5$, $0{\cdot}8$, 1 (curves 2–4, respectively). Curves 1–4 correspond to the rigorous equation (8); data 5 and 6—to the proposed approach equation (23) for $l = 0{\cdot}8$ and 1, respectively. $f_{L=0{\cdot}5} = 2V\tau_{L=0{\cdot}5}/\omega_x$ is the nondimensional duration of the signal measured at the level $L = 0{\cdot}5$ from the signal amplitude.

5.2. *Influence of the bandwidth limitation of a photoreceiver on the detected signal*

It is not difficult to show that, for most practical applications, when $r \leqslant \omega_x$ the shape of an undistorted signal may be estimated by the following approach:

$$k_{\mathrm{sh}}(t, l, s = 0, c) = \exp\left(-\tfrac{1}{2}(f\beta^{-1}_{L=0{\cdot}5}(l, s = 0, c))^2\right). \tag{23}$$

The coefficient of the pulse expansion $\beta_{L=0{\cdot}5}(l, s = 0, c) = f_{L=0{\cdot}5}(l, s = 0, c)/f_{L=0{\cdot}5}(l \to 0, s = 0, c)$ is presented in figure 9. For small particles (when $l \to 0$), equation (23) follows rigorously from equations (8) and (13). Figure 7

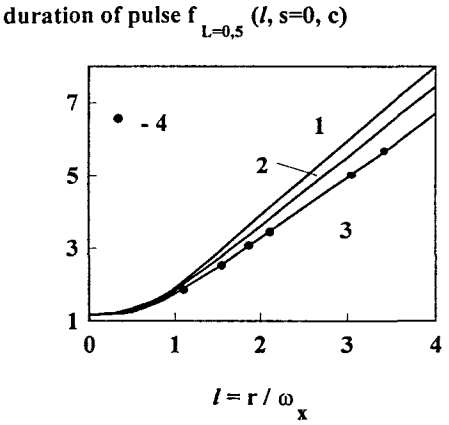

Figure 8. Theoretical (1–3) and experimental (4) [20] dependencies of the nondimensional duration $f_{L=0\cdot5}$ of a nondistorted signal due the parameter of a particle $l = r/\omega_x$ detected on the $L = 0\cdot5$ level of maximum amplitude. Curves 1–3 are plotted for $c = 1$, for $c = 2$, and for $c \geqslant 10$, correspondingly. Experimental results 4 are shown for $c = 24$.

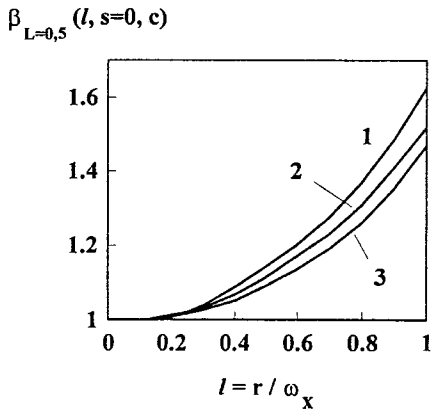

Figure 9. Variation of the signal parameter β as a function of the relative particle size: curves 1–3 correspond to $c = 1$, $c = 2$, $c \geqslant 10$.

illustrates good agreement between the rigorous results (curves 3, 4) and the corresponding data simulated by the proposed approach (curve 5 (open rectangles) and curve 6 (open circles)).

Taking into account equations (19) and (23), the following analytical expression is derived for the rapid engineering calculation of the distortion coefficient k_{ph}:

$$k_{\text{ph}}(t, l, s = 0, c) = \frac{1}{2} a \exp\left(\frac{a^2}{4\pi}\right) \exp(-\xi\alpha)\left[1 - 2\Phi_0\left(2^{1/2}\left|\frac{a}{2\pi^{1/2}} - \pi^{1/2}\xi\right|\right)\right], \quad (24)$$

where $a(l, s, c) = \tau_{\text{rec}}(l, s, c)/t_{\text{ph}}$ is the instrumental parameter;

$$\tau_{\text{rec}}(l, s, c) = \tau_{\text{rec}}(l \to 0, s, c)\beta_{L=0\cdot5}(l, s, c) \quad (25)$$

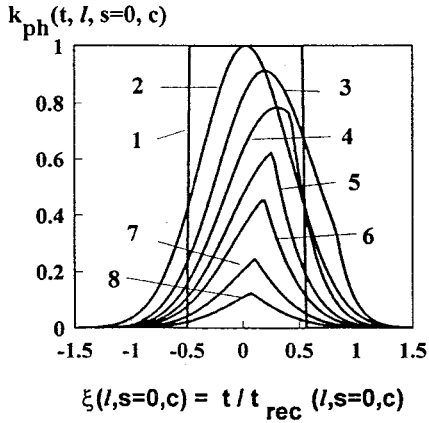

Figure 10. Time-dependent coefficient of the signal distortion caused by the bandwidth limitation of a photoreceiver: 1 is the equivalent rectangular pulse; 2 is the shape of an ideal nondistorted signal; 3–8 are actual normalized distorted signals for the instrumental parameter $a(l, s, c) = 5,\ 2{\cdot}5,\ 1{\cdot}5,\ 1,\ 0{\cdot}5,\ 0{\cdot}25$, respectively.

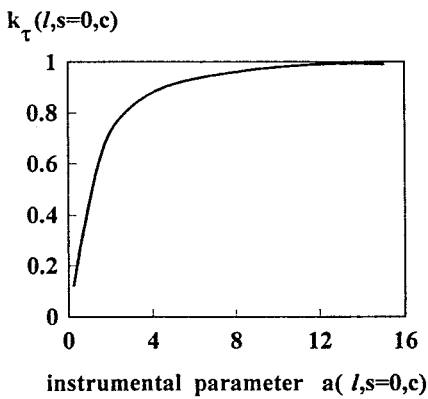

Figure 11. Coefficient of the pulse amplitude reduction allowing the estimation of the change of the response function of an analyser caused by the bandwidth limitation of a photodetector.

and

$$\tau_{\text{rec}}(l \to 0, s, c) = \left(\frac{\pi}{2}\right)^{1/2} \frac{\omega_x}{V} \tag{26}$$

are the duration of equivalent rectangular pulses having an amplitude and energy equal to the amplitude and energy of the nondistorted signals for particles with an arbitrary nondimensional radius l and $l \to 0$, respectively; $\xi(l, s, c) = t/\tau_{\text{rec}}(l, s, c)$ is the normalized nondimensional time; $\Phi_0(x) = (1/2\pi)^{0{\cdot}5} \int_0^x \exp(-z^2/2)\,dz$ is the normalized Laplace function. Figure 10 shows in relative units the equivalent rectangular pulse (curve 1), the ideal nondistorted signal (curve 2) and actual distorted signal (curves 3–8, which are calculated from equation 23 for the instrumental parameter $a(l, s, c) = 5, 2{\cdot}5, 1{\cdot}5, 1, 0{\cdot}5, 0{\cdot}25$, respectively). The coeffi-

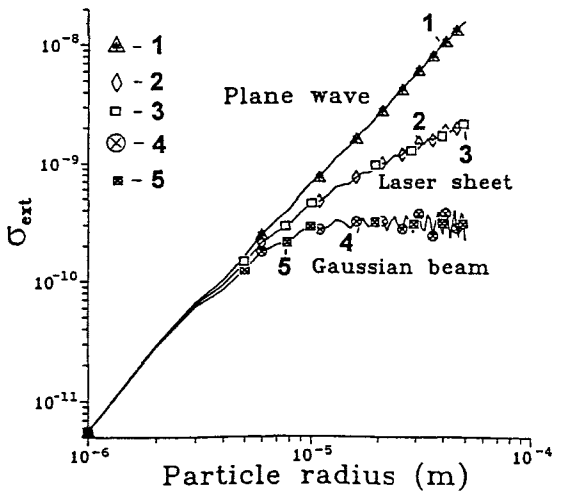

Figure 12. Comparison of extinction calibration characteristics of a particle analyser obtained by using the exact generalized Lorenz–Mie theory (curves 2 and 4) and the proposed modified plane-wave scattering approach (empty and filled squares). Curves 2 and 3 are obtained for the laser sheet ($2\omega_x = 20\,\mu m$; $2\omega_y = 200\,\mu m$) are borrowed from [10]. Curves 4 and 5 are plotted for the Gaussian beam ($2\omega = 2\omega_x = 2\omega_y = 20\,\mu m$). The curve 1 corresponds to points computed by using a plane wave program or a program for the laser sheet with large semi-axis $\omega_x = \omega_y = 500\,\mu m$ [10].

cient of the pulse amplitude reduction (see equation (21)) allowing for estimating the change of the response function of an analyser is given in figure 11. Thus, when the instrumental parameter $a(l, s, c)$ is more than 10, the above-mentioned distortion is negligible.

6. Comparison of the modified conventional plane-wave scattering approach and the Lorenz–Mie technique

6.1. *Extinction*

As an example of the practical significance of the proposed technique, we compare two pairs of curves: 2 and 3, 4 and 5, shown in the extinction diagram figure 12. These results were obtained for water droplets in air (the complex refractive index of particles is $m = 1{\cdot}33 - i0{\cdot}0$). The wavelength of the incident beam is $\lambda = 0{\cdot}5\,\mu m$. Curves 2, 3 correspond to the laser sheet ($2\omega_x = 20\,\mu m$, $2\omega_y = 200\ \mu m$). Curves 4 and 5 correspond to the circular Gaussian beam ($2\omega_x = 2\omega_y = 20\,\mu m$). Curves 2 and 4 ($\sigma_{ext\,Gaus}$) are calculated by using the exact generalized Lorenz–Mie theory and are borrowed from [10]. Curve 1 $\sigma_{ext\,plane}$ is obtained by the conventional plane-wave approach. Curves 3 and 5 are transformed from curve 1, taking into account Eq. (17). The transformation coefficient k_a is taken from figure 3 (curves 1 and 3).

As follows from the analysis of figure 12, curves 3 and 5, being the product of the proposed modified plane-wave approach, coincide well with the exact simulations (curves 2 and 4).

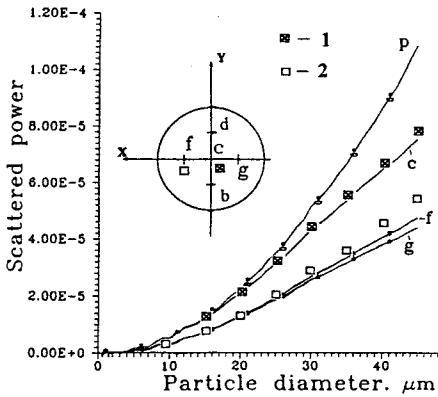

Figure 13. Near-forward scattering by particles with the different positions (b, c, d, f, and g) in the circular measurement volume of two intersected laser beams ($2\omega_x = 2\omega_x = 80\,\mu m$). Curve p corresponds to the plane-wave illumination. Curves p, c, f, g have been obtained by using the generalized Lorenz–Mie theory [11]. Results shown by filled and empty squares are transformed from the curve p by using the modified plane-wave scattering approach.

6.2. *Near-forward scattering*

Another comparison of the proposed simplified technique (filled and open squares) and the exact Lorenz–Mie theory (curves p, c, and f) is presented in figure 13 for the near-forward scattering by water droplets which interact with two intersecting beams in a phase Doppler anemometer described in [11]. The waist diameter of two circular laser beams is 80 μm and the laser wavelength is 0·6328 μm. Different droplet positions (f, g, b, and d), which are characterized by the same displacement from the centre c of the measurement volume, are also shown in figure 13. The centre of the rectangular receiving aperture is defined by an off-axis angle of 30° and an elevation angle of −1·27° (see figure 1). Curves p, c, f, and g are borrowed from [11]. The differences between the curves f and g (as well as between the curves b and d omitted here) are caused by the off-axis location of the receiving aperture and the dual beam illumination. These differences are discussed in detail, in [11]. The curve p is obtained for dual plane-wave scattering $P_{\text{sca plane}}(t = 0)$. Results shown by filled and empty squares $P_{\text{sca Gauss}}(t = 0)$) are transformed from the curve p, taking into account equation (5). The transformation coefficient k_a is taken from figure 4 (curves 1 and 3, respectively for $s = 0$ and $s = 1$). In spite of the dual-beam illumination scheme and the off-axis receiver location, curves 1 and 2 describe well the power scattered from an on- or off-axis particle (see the curves c and f, or g, respectively).

Good agreement between the results obtained by the exact technique and by the approach shown in figures 12 and 13 confirms the correctness and practical significance of the proposed technique for the rapid estimation of the influence of instrumental parameters of a single-beam analyser on its response functions.

However, the proposed technique cannot describe the influence of the phase effect on the electric field scattered in a dual-beam scheme when the elevation angle of a receiver centre deviates from zero. This is the reason why the technique

does not explain the difference between the curves f and g in figure 13 (as well as the extremely high difference between the curves b and d in figure 4, [11]).

7. Conclusions

Simplified technique for the rapid estimation of the influence of a Gaussian beam with an elliptical cross-section on the performance characteristics of a laser particle-size analyser is derived on the basis of the conventional plane-wave Mie scattering theory and the proposed assumption of the spectrum of plane-waves theory.

Correctness of the engineering technique for calculation of the attenuation, extinction, and near-forward scattering by particles is checked experimentally (see figure 8) and theoretically by comparison with the exact generalized Lorenz–Mie theory (see figures 12 and 13).

From a methodological point of view, the proposed technique includes only nondimensional coefficients: k_a, k_{sh}, k_{ph}, and k_τ.

It was shown that the coefficient k_a makes possible the estimation of the change of response functions in the range of particle diameters which are compared with the minor semi-axis $2\omega_x$ of a Gaussian beam (see figure 3). Coefficient k_{sh} describes the shape of a nondistorted pulsed signal (see figure 7). It can be used for the investigation of the second kind of response function which is the diameter-dependence of the signal duration (see figure 8).

Coefficients k_{ph} and k_τ show the influence of the bandwidth limitation of a photodetector on the shape of the signal (see figure 10) and on the response function in the range of particles with small diameters, respectively (see figure 11).

The proposed technique, being a rapid one, can be used effectively in the software of laser analysers for the automatic correction of results in real time measurements, if optical properties of measured particles differ from the optical properties of calibrated lattices.

The technique derived for the single-beam particle-size analyser is also valid for estimating the signal-pedestal amplitude in a dual-beam phase Doppler anemometer (see figure 13). However, the technique cannot explain the influence of the phase effect on the signal shape in a dual-beam analyser, especially if the elevation angle of the receiver aperture is different from zero.

The correct application of this technique to far-forward scattering requires additional research.

8. Acknowledgment

These research results were obtained with the assistance of the Alexander von Humboldt Foundation. V. I. Ovod is grateful to the staff of the Department of Process Engineering, University of Bremen, Germany for comprehensive discussions throughout the preparation of this paper.

References

[1] Leschonski, K., 1986, *Part. Part. Syst. Charact.* **3**, 99.
[2] Etzler, F. M., and Sanderson, M. S., 1995, *Part. Part. Syst. Charact.* **12**, 217.

[3] PETERS, C., and RUDOLPH, A., 1995, *Proceedings of the 4th International Congress on Optical Particle Sizing*, Nuerenberg, Germany, 21–23 March, p. 329.
[4] GIEL, T. V., HOLT, J. K., DOUGLAS, J. R., BONIN, M. P., and HOLVE, D. J., 1994, *Proceedings of the 32nd Symposium on Engineering Aspects of Magnetohydrodynamics*, Pittsburgh, PA, June, p. 1.
[5] GEBHART, J., and WESTENBERGER, S., 1995, *Proceedings of the 4th International Congress on Optical Particle Sizing*, Nuerenberg, Germany, 21–23 March, p. 21.
[6] LEE, H. S., Chae, S. K., and LIE, B. Y. H., *1989, Part. Part. Syst. Charact.* **6**, 93.
[7] OVOD, V. I., 1987, *Sov. J. Opt. Technol.*, **54**, 199.
[8] HEYDER, J., and GEBHART, J., 1979, *Appl. Optics*, **5**, 705.
[9] BOHREN, C. F., and HUFFMAN, D. R., 1983, *Absorption and Scattering of Light by Small Particles* (Wiley, New York), chap. 3.4, chap. 13.5.
[10] REN, K. F., GREHAN, G., and GOUESBET G., 1993, *Part. Part. Syst. Charact.* **10**, 146.
[11] GREHAN, G., GOUESBET, G., NAQWI, A., and DURST, F., 1993, *Part. Part. Syst. Charact.* **10**, 332.
[12] LOCK, J. A., 1995, *Appl. Opt.*, **34**, 559.
[13] LOCK, J. A., and HODGES, J. T., 1996, *Appl. Opt.* **35**, 6605.
[14] KHALED, E. E. M., HILL, S. C., and BARBER, P. W., 1993, *IEEE Trans. Antennas Propagat.* **41**, 295.
[15] OVOD, V. I., and WRIEDT, T., 1994, *Proc. of the Sixth International Conference on Liquid Atomization and Spray Systems*, Rouen, France, July, p. 491.
[16] OVOD, V. I., 1995, *Part. Part. Syst. Charact.*, **12**, 207.
[17] OVOD, V. I., 1995, *Part. Part. Syst. Charact.*, **12**, 42.
[18] OVOD, V. I., August 1996, *Scientific Report*, (Brussels: Department of Theoretical Physical Chemistry, Vrije Universiteit Brussel).
[19] HIRLEMAN, E. D., and STEVENSON, W. H., 1978, Appl. Optics, **17**, 3496.
[20] STEINKAMP, J. A., HANSEN, K. M., and CRISSMAN, H. A., 1976, *J. Histochem. Cytochem.*, **24**, 291.